Quadrupole alignment studies in the HRSs

L.Pentchev, J.LeRose, and the FPP collaboration

The main goal of these studies is to reduce to systematic error in the measurements of the ratio $r = \mu G_e/G_m$ (E-99-007) due to uncertainties in the absolute value of the proton bend angle $\Delta\phi$ in the non-dispersive plane of the spectrometer. In dipole approximation this systematic error is estimated by:

$$\Delta r = \mu \frac{(E+E')}{2m} tg\left(\frac{\theta}{2}\right)\gamma\left(\frac{g}{2}-1\right)\Delta\phi \tag{1}$$

where E, E', and θ are the electron initial, final energy, and angle; m, γ, g – proton mass, γ factor, and gyro-magnetic ratio. For example, for the highest q^2 of E-99-007, $5.6GeV^2$, we estimate that $\Delta\phi = 1.4mrad$ [1] in the left arm used in the experiment. Then we have $\Delta r = 0.041$, to be compared with the absolute statistical error of 0.085 for this kinematics. In addition, a procedure for precise measurement and on-line calibration of the target y-position (y_{targ}) with respect to the spectrometer axis, is proposed.

To investigate possible misalignment of the magnetic elements in the non-dispersive plane which may bend the central trajectory, we performed measurements with 7 different settings of the spectrometers. The test was done simultaneously for both arms looking at the elastic scattering of a $0.836GeV$ electron beam on a carbon target at 15^0 with sieve slits.

$Name$	$Q1$	$Q2$	$Q3$	$(y\|y_{tg})$	$(y\|\phi_{tg})$	$(\phi\|y_{tg})$	$(\phi\|\phi_{tg})$
nom.	1	1	1	-0.625	-0.812	0.358	-1.133
"q1"	-1.117	0	0	-26.57	0.430	-2.316	0.000
"q2"	0	0.815	0	-9.352	1.194	-0.840	0.000
"q3"	0	0	0.368	2.749	40.90	-0.024	0.000
"q1r"	0.7	1	1	-0.717	-1.010	0.717	-0.385
"q2r"	1	0.7	1	0.098	1.411	-1.098	-5.603
"q3r"	1	1	0.7	-1.546	0.945	0.149	-0.738

Table 1: Different quadrupole settings used in the test given as correction factors to the standard tune, and the first order optics coefficients in the non-dispersive plane calculated with COSY (TRANSPORT gives very similar results)

Besides the standard tune of the spectrometers, we have used 3 settings with only one of the quadrupoles and the dipole energized in which case the

[1] this is the angle of the central trajectory with respect to the VDC ($p000$ coefficient in ESPACE) assuming that the VDC angle ϕ_0 is close to zero (see table3 later)

quadrupole current was chosen to give point-to-parallel focusing in y direction ($(\phi|\phi_{tg}) = 0$), and another 3 settings in which the current in one of the quadrupoles was reduced by 30% from the standard value (table 1) [2].

By systematically changing the spectrometer settings, we hoped to interpret the observed movements of the image of the central sieve slit hole on the focal plane as the result of misalignment of the magnetic elements. The identification of the central hole image and the elastic peak is important in order to minimize the contributions from the higher order terms and to reduce the correction for ϕ_{tg}. For this purpose, we simulated the above spectrometer settings with the COSY code taking into account the multiple scattering in the material at the target region. It turns out that one can easily identify the central hole and the elastic peak for the "q1r", "q2r", and "q3r" settings, which do not differ significantly from the nominal setting.

For the "q1", "q2", and "q3" setting, the data and simulations for the left arm are compared in figures 1 and 2. The results for the right arm are similar, except for the difference shown in figure 3.

In the case of "q2" and "q3", one can separate the holes vertically using plots of θ vs x at the focal plane (figure 1). From the same plots the elastic peak is separated from the excitation peaks. The ability to separate the holes horizontally are demonstrated in figure 2. In the simulation results for the "q1" and "q2" settings different lines in the plot correspond to different holes in the central row. In the case of "q3" we observe only the image of the central hole, for the other holes the y-coordinate is outside the VDC. For all the settings ϕ distributions appear to be much broader in the data than in the simulations. Values of several *mrad* for the R.M.S. cannot be explained by the VDC resolution or multiple scattering in the focal plane. It seems that the spectrometer model used in COSY, is good enough for the nominal tune (figure 2), but not for completely different magnet configurations with significant magnification in y (table 1). Nevertheless, for the "q2" setting by comparing with the simulations, we associate the central spot in the plot of figure 2 as corresponding to the central hole. This assumption is consistent with the other measurements, as discussed later.

In the case of "q1", it is problematic to identify the elastic peak (figure 1) and the different horizontal holes cannot be separated (figure 2), therefore, we have chosen not use this setting in the analysis.

The measured peak positions of y and ϕ at the focal plane that correspond to the central hole in the sieve slit, are shown in table 2. For the "q3" setting the acceptance in y is limited by the $15cm$ opening at the exit of the vacuum box. Since the trajectories after the Q3 magnet are parallel within few milliradians, one can observe this $15cm$ directly by looking at the y distribution at the focal plane (figure 3). In case of the right arm, the peak position is outside the opening. The corresponding value in table 2 in this case is the peak position of

[2] **the units in this report are always mm and mrad**

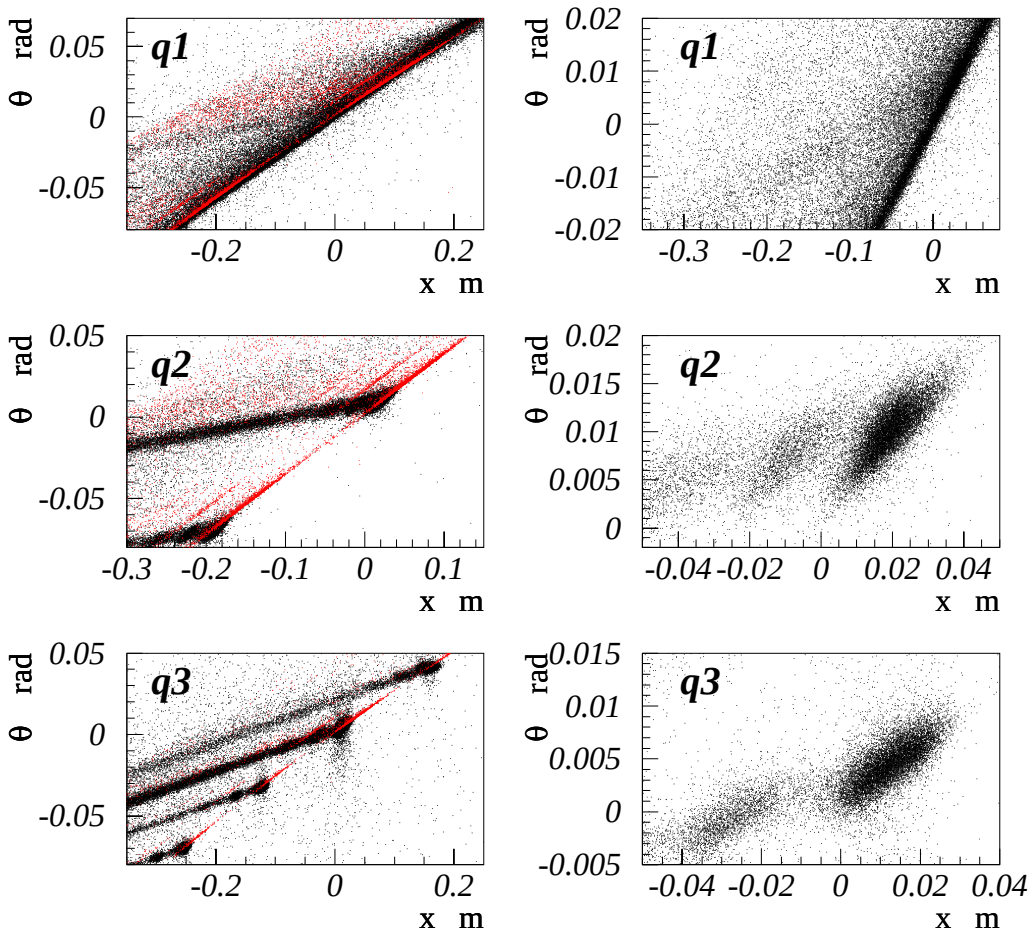

Figure 1: Left panel: Data (black) compared with the simulations (red) in terms of x and θ at the focal plane for the settings as indicated in case of the left arm; different strips (in horizontal direction) correspond to holes with different θ_{targ}. Right panel: only the data for the central row of sieve slit holes, magnified; different spots correspond to (from the right to the left) elastic and excitation peaks.

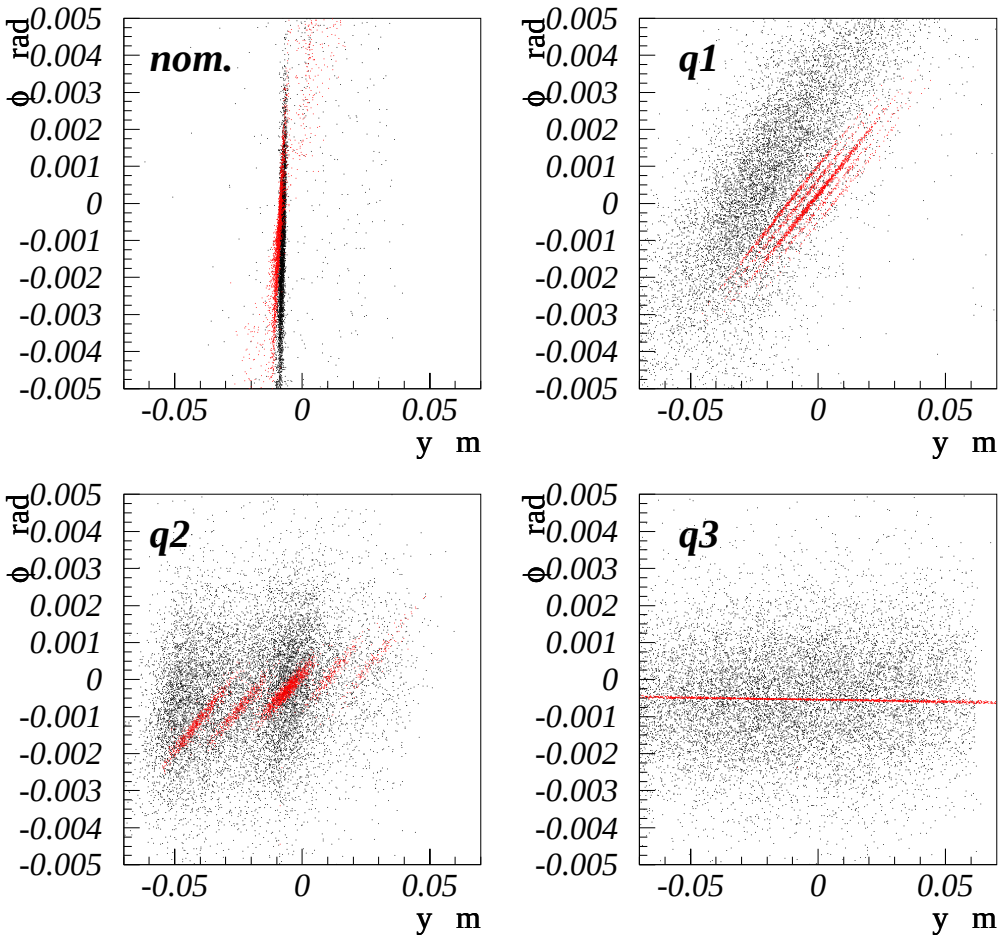

Figure 2: Data (black) compared with the simulations (red) in terms of y and ϕ at the focal plane for the settings as indicated in case of the left arm. Only the elastic events and the central row of holes are selected from figure 1. Note, the scale is the same for all the plots.

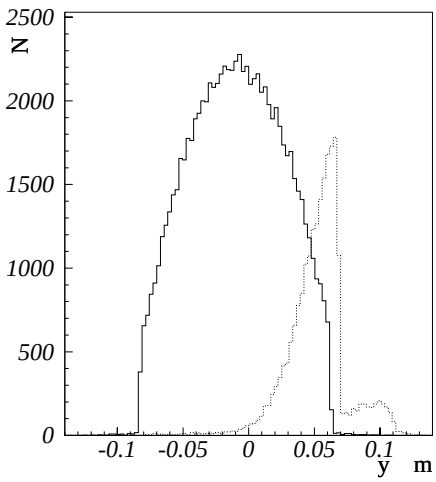

Figure 3: Distributions of y at the focal plane for the left (solid) and right (dotted) arm for the "q3" setting.

the small bump at the right side in figure 3 that represents events with electrons scattered in the material next to the opening.

We consider a shift, s_i, and rotation at angle a_i (about the middle entrance point) in the non-dispersive plane of the i-th quadrupole with respect to the dipole axis. The effect of these misalignments on ϕ and y at the focal plane is calculated with both the COSY and TRANSPORT codes in terms of the derivatives $(\phi|s_i) = d\phi/ds_i$, $(\phi|a_i) = d\phi/da_i$, $(y|s_i) = dy/ds_i$, and $(y|a_i) = dy/da_i$. In first order the measured peak positions are given by:

$$\begin{aligned}
\phi &= \phi_0 + (\phi|y_{tg})y_{tg} + (\phi|\phi_{tg})\phi_{tg} + \sum_{i=1}^{3}(\phi|s_i)s_i + \sum_{i=1}^{3}(\phi|a_i)a_i \\
&= \phi_0 + \{(\phi|y_{tg}) - (\phi|\phi_{tg})/z_{hole}\}y_{tg} + (\phi|\phi_{tg})y_{hole}/z_{hole} \\
&\quad + \sum_{i=1}^{3}(\phi|s_i)s_i + \sum_{i=1}^{3}(\phi|a_i)a_i \qquad (2) \\
y &= y_0 + (y|y_{tg})y_{tg} + (y|\phi_{tg})\phi_{tg} + \sum_{i=1}^{3}(y|s_i)s_i + \sum_{i=1}^{3}(y|a_i)a_i \\
&= y_0 + \{(y|y_{tg}) - (y|\phi_{tg})/z_{hole}\}y_{tg} + (y|\phi_{tg})y_{hole}/z_{hole}
\end{aligned}$$

$$+\sum_{i=1}^{3}(y|s_i)s_i+\sum_{i=1}^{3}(y|a_i)a_i \tag{3}$$

where y_0 and ϕ_0 are the VDC coordinate and angle offsets with respect to the dipole axis, z_{hole} is the distance between the target and the sieve slit, and y_{hole} is the y-coordinate of the central hole. The above equations written for each setting used in the analysis result in a set of 12 equations. Since, the effects of the shifts and rotations of each quadrupole are very similar for all the settings: $(y|s_i) \sim (y|a_i)$, the shifts cannot be separated from the rotations with any reasonable precision. Therefore, when solving the above equations, we will consider either s_i as unknowns and $a_i = 0$, or a_i as unknowns and $s_i = 0$.

Name	left arm		right arm	
	ϕ	y	ϕ	y
nom.	-1.324 ± 0.017	-7.720 ± 0.014	-4.820 ± 0.021	-5.157 ± 0.015
"q2"	-0.192 ± 0.011	-5.928 ± 0.077	2.162 ± 0.017	26.445 ± 0.084
"q3"	-0.481 ± 0.008	-9.362 ± 0.477	-0.406 ± 0.011	94.106 ± 0.557
"q1r"	-1.199 ± 0.014	-7.676 ± 0.033	-3.613 ± 0.017	-5.446 ± 0.016
"q2r"	-0.836 ± 0.050	-7.943 ± 0.021	-13.86 ± 0.056	-0.953 ± 0.013
"q3r"	-0.808 ± 0.024	-6.169 ± 0.015	-2.951 ± 0.013	3.082 ± 0.014

Table 2: Measured peak positions of ϕ and y focal plane for the different settings and arms.

The values of z_{hole} and y_{hole} are known with very good precision, while the results for y_{tg} as surveyed immediately after the test [1] (corrected for the warm up and vacuum motion of the target and the beam position) and for y_0 and ϕ_0 surveyed five years ago, are summarized in tables 3 and 4. First, we assume that y_{tg} is known with a precision of $0.5mm$. We consider y_0, ϕ_0, and s_i (or a_i) $(i = 1, 2, 3)$ as 5 unknowns, which can be calculated from the above 12 equations using the linear least squares method. In this case however, the variation of the result for y_0 due to the uncertainty of y_{tg}, is about $25mm$ (tables 3 and 4). This is due to the strong correlation: $y_0 \approx -50y_{tg} + const$, which is mainly a result of the significant magnification in y (table 1) in the case of the "q3" setting.

Therefore, it is much better to use the y_0 value from the survey assuming conservatively an uncertainty of $3mm$ and consider y_{tg}, ϕ_0, and s_i (or a_i) as unknowns. The values of χ^2/N for such a fitting procedure are, however, too high - about 160/7 for the left arm and 500/7 for the right arm. The poor quality of the fit is an indication that the statistical errors - most of all of the order of several hundredths of mm and $mrad$ (table 2) - are smaller than the systematic errors, associated with the model uncertainties in the derivatives in equations (2,3) and the contribution from terms of order higher than one. A big advantage for the left arm measurement is the fact that y_{targ} was very close to zero (table 3) that makes the target corrections and, correspondingly, the model

	ϕ_0	y_{targ}	y_0
survey	-0.05 ± 0.3	0.078	-9.1 ± 0.26
this report	-0.567 ± 0.305	0.035 ± 0.206	-9.50 ± 25.24
ESPACE	—	-0.300	—

Table 3: Comparison of different results for ϕ_0, y_{targ}, and y_0 for the left arm. ϕ_0 and y_{targ} of this report are obtained by using y_0 from the survey, the systematic errors given are calculated assuming uncertainties of $3mm$ in y_0 and $0.1mm$ in y_{hole}; while y_0 – by using the survey result for $y_{targ} \pm 0.5mm$. For the survey results, only the statistical errors are given estimated from several measurements done at different VDC points.

	ϕ_0	y_{targ}	y_0
survey	—	-2.177	-2.7
this report	-0.218 ± 0.346	-2.012 ± 0.359	-11.00 ± 25.52
ESPACE	—	-2.280	—

Table 4: Same as table 3 but for the right arm.

errors due to these corrections, negligible. This explains the lower χ^2/N values for the left arm. However, the model uncertainties in the derivatives $(\phi|s_i)$, $(\phi|a_i)$, $(y|s_i)$, and $(y|a_i)$ still remain and contribute to the poor fit quality for both arms.

To estimate the effect of the systematic errors, we have done a two-step minimization - first, taking into account in the weights w_ϕ and w_y of the equations (2,3) only the statistical errors σ_ϕ and σ_y, and second, using in addition the first order corrections due to the non-zero central hole and target positions, and quadrupole shifts (or rotations), assuming 10% model errors for the derivatives:

$$\begin{aligned} 1/w_\phi^2 &= \sigma_\phi^2 + [0.1(\phi|\phi_{tg})y_{hole}/z_{hole}]^2 + [0.1\{(\phi|y_{tg}) - (\phi|\phi_{tg})/z_{hole}\}y_{tg}]^2 \\ &\quad + \sum_{i=1}^{3} [0.1(\phi|s_i)s_i]^2 \qquad (4) \\ 1/w_y^2 &= \sigma_y^2 + [0.1(y|\phi_{tg})y_{hole}/z_{hole}]^2 + [0.1\{(y|y_{tg}) - (y|\phi_{tg})/z_{hole}\}y_{tg}]^2 \\ &\quad + \sum_{i=1}^{3} [0.1(y|s_i)s_i]^2 \qquad (5) \end{aligned}$$

where the values of y_{tg} and s_i (or a_i) are calculated in the first step. Thus, increasing the errors, more significantly for the right arm, we typically get $\chi^2/N = 7/7$ to $20/7$ for the left arm and about $3/7$ for the right arm.

The result for the fitted parameters ϕ_0, y_{tg}, and s_i (or a_i) as a function of

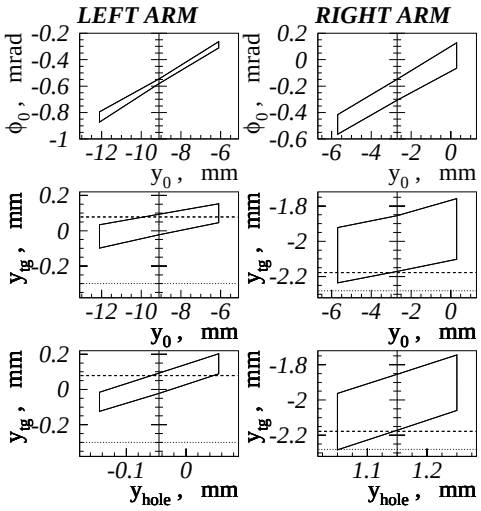

Figure 4: Ranges of the VDC angle ϕ_0 and target position y_{targ} as a function of the VDC position y_0 and central hole position y_{hole} for the left and right arm using COSY. The vertical scales in the center of the plots are located at the survey values of y_0 and y_{hole}. The horizontal dashed lines indicate y_{tg} from the survey, and the dotted lines are the ESPACE result.

y_0 when using the COSY model are shown in figures 4, 5, and 6. The ranges shown include, in addition to the error of the minimization, the variations of the parameters from the first to the second step, and their change when assuming only shifts or only rotations of the quadrupoles. In addition the dependence of y_{tg} on the position of the central hole y_{hole} is shown at figure 4, while the other parameters are almost independent on y_{hole}. Table 5 summarizes the total ranges of the fitted parameters. The procedure was repeated using the derivatives calculated with the TRANSPORT code. Comparing with the COSY calculations (table 5), there is some visible difference only for the right arm due to the more significant target corrections.

In case of the left arm the y_{targ} obtained from the fit is in excellent agreement with the survey result (table 3, figure 4). In addition to the $3mm$ uncertainty of y_0, if we assume a $0.1mm$ uncertainty of the central hole position y_{hole}, we can reconstruct y_{targ} with a systematic error of 0.2 which is much below the errors stated for the other methods of measurement. As explained before, the success of the present method is due to the y-magnification for the "q3" setting. As a simple example, one can see in figure 3 a huge difference, about $10cm$, between the y-peak positions for the left and right arm, which corresponds to a difference in y_{targ} of only $2.25mm$. In addition, the peak positions for the "q3"

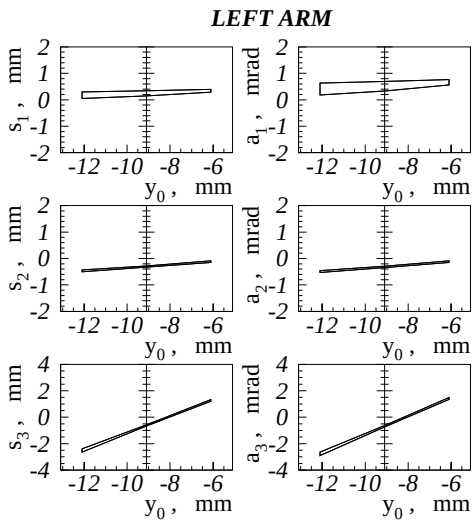

Figure 5: Ranges of the shifts s_i and angle offsets a_i of the quadrupoles as a function of the VDC position y_0 for the left arm using COSY. The fits for s_i and a_i were done separately assuming only shifts or only angle offsets. The vertical scales in the center of the plots are located at the survey value of y_0.

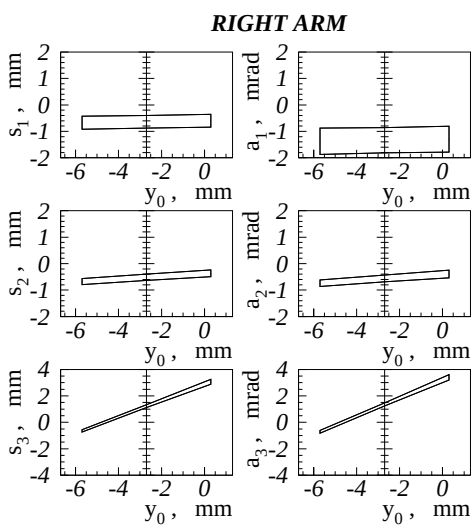

Figure 6: Same as figure 5 but for the right arm.

setting depend very weakly on possible quadrupole offsets and since big offsets are excluded from the other measurements, their contribution is negligible.

Name	left arm		right arm	
	COSY	TRANSPORT	COSY	TRANSPORT
ϕ_0	-0.567 ± 0.305	-0.567 ± 0.305	-0.218 ± 0.346	-0.230 ± 0.345
y_{tg}	0.035 ± 0.206	0.035 ± 0.204	-2.012 ± 0.359	-2.016 ± 0.364
s_1	0.221 ± 0.170	0.221 ± 0.169	-0.639 ± 0.281	-0.577 ± 0.272
s_2	-0.296 ± 0.207	-0.292 ± 0.203	-0.516 ± 0.282	-0.505 ± 0.269
s_3	-0.655 ± 1.984	-0.662 ± 1.987	1.260 ± 1.994	1.219 ± 1.997
a_1	0.473 ± 0.289	0.472 ± 0.292	-1.339 ± 0.530	-1.214 ± 0.516
a_2	-0.308 ± 0.222	-0.306 ± 0.221	-0.558 ± 0.309	-0.545 ± 0.295
a_3	-0.710 ± 2.195	-0.720 ± 2.197	1.396 ± 2.214	1.346 ± 2.215

Table 5: Total ranges of the fitted parameters: VDC angle ϕ_0, target position y_{targ}, shifts s_i and angle offsets a_i of the quadrupoles, using the survey results for y_0 and y_{hole} (tables 3, 4) and assuming $\pm 3mm$ error for y_0 and $\pm 0.1mm$ error for y_{hole}, calculated with COSY and TRANSPORT for the left and right arm. The fits for s_i and a_i were done separately assuming only shifts or only rotations - i.e. when modeling the spectrometers one can use either shifts or rotations, but not both.

Similar considerations are valid for reconstructing ϕ_0. Again the most informative is the "q3" setting, in which case the ϕ-peak corrected by the target position defines the ϕ_0 value. Since the target position is reconstructed with very good precision, one can reconstruct ϕ_0 with a systematic error of $0.3mrad$ defined mainly by the $3mm$ uncertainty in y_0. According to equation (1) such uncertainty reduces the systematic error of the ratio down to $\Delta r = 0.009$.

The entire set of data for the left arm can be explained by quadrupole offsets less than $0.5mm$ or $0.8mrad$, except for a possible Q3 misalignment of maximum $2.5mm/3mrad$. Theoretically, it is possible to have a special relation between the shift and rotation for a given quadrupole so that their effects cancel, in which case the offsets can be bigger. However, it is very unlikely that the quadrupoles have been positioned in such a special way.

In the case of the right arm, the most important difference is that the corrections for the non-zero target position are dominant. In addition (and as a result of the target position) the y-peak for the "q3" setting, which is very important for the whole reconstruction procedure as explained above, was outside the vacuum box opening. All this introduces systematic errors and reduces the fit quality. In particular, the result for y_{targ} (table 4) is affected directly by the error of the y-peak position. Despite these problems, the data can be explained with offsets of Q1 and Q2 of about $1mm$ or $2mrad$ and Q3 offset of no more than $3mm/3.5mrad$ (figures 4, 6 and table 5).

Procedure for a precise measurement of y_{targ}

We suggest an alternate procedure for measuring the target position, using a single arm and the "q3" setting. The method is based on the significant angle to y-coordinate magnification in this setting that makes possible the reconstruction of ϕ_{tg} with high precision. Since, y_{hole} is known with good accuracy, one can reconstruct y_{targ} also with high precision.

According to equation (3) and considering for example only shifts:

$$y_{targ} = \frac{y - y_0 - (y|\phi_{tg})y_{hole}/z_{hole} - (y|s_3)s_3}{(y|y_{tg}) - (y|\phi_{tg})/z_{hole}} \tag{6}$$

Important is that the big value of $(y|\phi_{tg})$ (table 1) in the denominator of (6) reduces the systematic error of y_{targ} due to uncertainties in y_0, y_{hole} and y, to a very low level. To eliminate the systematic error due to the model uncertainty of $(y|\phi_{tg})$, one can adjust the peak of the y-distribution at the focal plane by changing the beam position, so that y_{targ} equals y_{hole}:

$$y = y_0 + (y|y_{tg})y_{hole} + (y|s_3)s_3 \tag{7}$$

using the values of y_0, s_3, and $(y|y_{tg})$ from this report, and $(y|s_3) = -0.518$. The above choice makes the result for y_{targ} (6) independent of $(y|\phi_{tg})$.

Thus, the procedure consist of the following steps:

- Survey of y_{hole}
- By changing the beam position horizontally, adjust the peak position of the y-distribution at the VDC to the value of (7). For this beam position $y_{targ} = y_{hole}$.
- Measure the beam position
- Move the beam back to the standard position and measure it. y_{targ} for this beam position can be calculated geometrically from the above measurements.

To estimate the systematic error, we use the results of this report for s_3 as correlated with the value of $y_0 \pm 3mm$ (figures 5,6). In addition we assume $0.1mm$ error for the position of the central hole y_{hole}, $0.5mm$ – for the measured value of y, and 10% model uncertainty for each of the derivatives in (6). Thus, the total systematic error is $0.183mm$ for the left and $0.193mm$ for the right arm, dominated by the error due to the uncertainty in y_{hole} ($0.11mm$) and in y_0 ($0.06mm$).

Conclusions

The entire set of the data for the left arm can be explained by quadrupole offsets less than $0.5mm$ or $0.8mrad$, except for Q3 for which offsets up to $2.5mm/3mrad$ are possible. This is in agreement with the stated precision of the quadrupole positioning. The obtained value for the VDC angle offset ϕ_0 with a systematic error of $0.3mrad$ makes possible calculation of the $\mu G_e/G_m$ ratio (E-99-007) with a significantly reduced systematic error (0.009 for the highest q^2) due to uncertainties in the proton bend angle $\Delta\phi$.

The results for the right arm are less conclusive due to the relatively big value of y_{targ} in this case, which introduces significant systematic uncertainties. Nevertheless, one can state that drastic offsets of more than few mm or $mrad$ are excluded.

The model dependence (COSY or TRANSPORT) of the results is weak, however, all the models have problems in describing the focal plane distributions for the "Dipole + one quadrupole" configurations.

The "Dipole+Q3" setting can be used for reconstructing y_{targ} with a systematic error less than $0.2mm$ which is much better than any other previously used method. Even more, one can use this setting for a fine on-line adjustment of y_{targ} for one of the arms, by changing the beam position.

If the results presented here for the right arm are not satisfactory, one should consider new measurements in which y_{targ} for this arm is adjusted to zero.

References

[1] JLab Alignment Group, April 2001, data transmittal # A665, A668, A669.